HHS Public Access

Author manuscript

Abdom Radiol (NY). Author manuscript; available in PMC 2018 December 01.

Published in final edited form as:

Abdom Radiol (NY). 2017 December ; 42(12): 2843–2854. doi:10.1007/s00261-017-1206-4.

Repeatability and Reproducibility of 2D and 3D Hepatic MR Elastography with Rigid and Flexible Drivers at End Expiration and Inspiration in Healthy Volunteers

Kang Wang, MD, PhD[1], **Paul Manning, MD, MS**[1], **Nikolaus Szeverenyi, PhD**[1], **Tanya Wolfson, MA**[3], **Gavin Hamilton, PhD**[1], **Michael S. Middleton, MD, PhD**[1], **Florin Vaida, PhD**[4], **Meng Yin, PhD**[2], **Kevin Glaser, PhD**[2], **Richard L. Ehman, MD**[2], and **Claude B. Sirlin, MD**[1]

[1]Liver Imaging Group, Department of Radiology, University of California, San Diego, School of Medicine, San Diego, CA

[2]Department of Radiology, Mayo Clinic, Rochester, MN

[3]Computational and Applied Statistics Laboratory (CASL), SDSC, University of California, San Diego, La Jolla, CA

[4]Division of Biostatistics and Bioinformatics, Department of Family Medicine and Public Health, University of California, San Diego, La Jolla, CA

Abstract

Purpose—To evaluate the repeatability and reproducibility of 2D and 3D hepatic MRE with rigid and flexible drivers at end expiration and inspiration in healthy volunteers.

Material and Methods—Nine healthy volunteers underwent two same-day MRE exams separated by a 5–10 minute break. In each exam, 2D and 3D MRE scans were performed, each under four conditions (2 driver types [rigid, flexible] × 2 breath-hold phases [end-expiration, end-inspiration]). Repeatability (measurements under identical conditions) and reproducibility

Corresponding Author Info: Kang Wang, M.D., Ph.D., Liver Imaging Group, Department of Radiology, University of California, San Diego, School of Medicine San Diego, CA, Address: MR-3T Research Building, 408 Dickinson Street, San Diego, CA, 92103-8226, Telephone: 415-812-3683, Fax: 619-471-0503, kaw016@ucsd.edu.

Conflict of Interests:

Author Kang Wang, Paul Manning, Nikolaus Szeverenyi, Tanya Wolfson, Gavin Hamilton, Florin Vaida has nothing to disclosure.
Author Michael S. Middleton discloses the following: Consultant, Allergan, Inc. Institutional research contract, Bayer AG Institutional. Research contract, Sanofi-Aventis Group. Institutional research contract, Isis Pharmaceuticals, Inc. Institutional research contract, Johnson & Johnson. Institutional research contract, Synageva BioPharma Corporation. Institutional research contract, Takeda Pharmaceutical Company Limited. Stockholder, General Electric. Company Stockholder, Pfizer Inc. Institutional research contract, Pfizer Inc.
Author Meng Yin discloses the following: intellectual property rights and financial interest in MRE technology.
Author Kevin Glaser discloses the following: intellectual property rights in MRE technology, Stockholder in Resoundant Inc.
Author Richard Ehman discloses the following: CEO, Resoundant Inc.
Stockholder, Resoundant Inc. Research Grant, Resoundant Inc.
Author Claude Sirlin discloses the following: Research Grant, General Electric. Company Research Grant, Siemens AG. Research Grant, Guerbet SA.

Compliance with Ethical Standards:

Ethical approval: All procedures performed in studies involving human participants were in accordance with the ethical standards of the institutional and/or national research committee and with the 1964 Helsinki declaration and its later amendments or comparable ethical standards.
Informed consent: Informed consent was obtained from all individual participants included in the study.

(measurements under different conditions) were analyzed by calculating bias, limit of agreement, repeatability coefficient (RC), reproducibility coefficient (RDC), intraclass correlation coefficient (ICC), and concordance correlation coefficient (CCC), as appropriate.

Results—For 2D MRE, RCs and ICCs range between 0.29 – 0.49 and 0.71 – 0.91, respectively. For 3D MRE, RCs and ICCs range between 0.16 – 0.26 and 0.84 – 0.96, respectively. Stiffness values were biased by breath-hold phase, being higher at end-inspiration than end-expiration, and the differences were significant for 3D MRE ($p < 0.01$). No bias was found between driver types. Inspiration-vs.- expiration RDCs and CCCs ranged between 0.30–0.54 and 0.61–0.72, respectively. Rigid-vs.-flexible driver RDCs and CCCs ranged between 0.10–0.44 and 0.79–0.94, respectively.

Conclusion—This preliminary study suggests that 2D MRE and 3D MRE under most conditions potentially have good repeatability. Our result also points to the possibility that stiffness measured with the rigid and flexible drivers is reproducible. Reproducibility between breath-hold phases was modest, suggesting breath-hold phase might be a confounding factor in MRE-based stiffness measurement. However, larger studies are required to validate these preliminary results.

Keywords

MR elastography; repeatability; reproducibility; flexible driver; rigid driver; 2D-MRE; 3D-MRE; quantitative imaging biomarker; QIB; QIBA; liver

INTRODUCTION

Magnetic resonance elastography (MRE) is an MR-based imaging technique used to estimate tissue stiffness. In MRE, a mechanical excitation driver is applied to tissue and harmonic vibration is generated which creates shear waves through the tissue[1]. The shear waves are visualized using phase-contrast MRI, and tissue stiffness is estimated by analyzing the propagation of the shear waves [2,3]. Liver stiffness measured with hepatic MRE is emerging as a leading quantitative imaging biomarker (QIB) for hepatic fibrosis [4–8]. Numerous cross-sectional studies have shown that MRE accurately assesses hepatic fibrosis noninvasively in a variety of chronic liver diseases using histology as the reference standard [4,5,9], and there is growing interest in using MRE to monitor hepatic fibrosis changes longitudinally[10]. However, before MRE can be implemented more widely in research and clinical settings, precision (repeatability and reproducibility) of MRE must be assessed [11,12].

Although the precision of hepatic MRE has been assessed in human subjects previously, most prior studies have focused on a single variant of MRE [13–17]. This variant generates shear waves using a rigid driver and performs image acquisition at end-expiration using a gradient recalled echo (GRE) MRE sequence [4,18]. Typically 2–4 axial slices depicting the through-plane component of the tissue motion are measured, the acquired waves images are processed by a two-dimensional direct inversion algorithm (2D MRE) to estimate a stiffness map (elastogram) of the liver, a region of interest (ROI) is placed on the elastogram, and a final average liver stiffness value is calculated as the QIB [4,13,14]. Although this variant

provides high accuracy for diagnosis of hepatic fibrosis, newer MRE sequence, inversion algorithm, and driver design are being developed to further improve this technology [4,7,19].

For example, a recent development is a spin-echo echo-planar (SE-EPI) MRE sequence that has fast scan time, allowing rapid data acquisition of the x, y, and z components of the vector tissue motion over a large volume of the liver in a reasonable time [20,21]. This allows for data processing using a 3D vector-based inversion algorithm. The tissue stiffness estimation based on this 3D MRE method is more robust and accurate than 2D scalar MRE because it requires fewer assumptions about the polarization and propagation direction of the waves and thus can handle more complex shear wave motion in organs with complicated shapes such as the liver and pancreas [20,22–24]. The precision of 3D MRE in the liver has yet to be examined in detail.

Additionally, the rigid driver used in most published studies to date can be uncomfortable for some patients, thus an ergonomic, flexible, prototype driver has been developed recently [19]. Compared to the rigid driver, the flexible driver is more comfortable and, by better conforming to body curvature, may produce more uniform shear waves, potentially further improving hepatic stiffness estimation accuracy [19]. The repeatability of this flexible driver prototype has only been evaluated in one study with 2D MRE [25]. Finally, although it is recommended that MRE be performed at end expiration, some individuals cannot hold their breath comfortably in expiration and may require end-inspiratory scanning. The effect of breath-hold phase on MRE measurements and the precision of end-inspiratory MRE have been under examined and have only been reported for the standard 2D MRE [26]. Thus, despite the compelling evidence for validation of MRE for assessing hepatic fibrosis, gaps in knowledge remain, especially for MRE variants.

The objective of this pilot study was to evaluate the repeatability and reproducibility of 2D and 3D hepatic MRE with rigid and flexible drivers at end expiration and inspiration in healthy volunteers. Because accuracy of MRE hepatic stiffness estimation depends on shear wave image quality, we also assessed the wave-image quality of 2D and 3D MRE under these conditions. We did not attempt to assess the reproducibility between 2D and 3D MRE since the inversion algorithms are quite different and it is known that 2D MRE slightly overestimates the stiffness relative to 3D MRE [22,27].

MATERIALS AND METHODS

Experimental Design

Our institutional review board (IRB) approved this Health Insurance Portability and Accountability Act (HIPAA)-compliant study. Nine healthy adult volunteers with no known liver disease were enrolled: five women and four men, mean age 28 years, range 24 – 37 years; mean BMI 25 kg/m^2, range 19 – 31 kg/m^2. Subjects provided signed informed consent and underwent two same-day MRE exams. Between exams, subjects were removed for five to ten minutes, and then repositioned on the scanner table. In each exam, 2D and 3D MRE scans were performed, each under four conditions (2 driver types [rigid, flexible] × 2 breathhold phases [end-expiration, end-inspiration]).

MRE Exams

All MRE exams were performed on a 3T MRI scanner with commercially available software and hardware (GE Healthcare, Waukesha, WI and Resoundant Inc., Rochester, MN) [4]. Subjects were instructed to fast for at least four hours before the first session to reduce possible confounding physiological effects, and were positioned supine, feet first, with a torso phased-array coil centered at the level of the liver. A dielectric pad was placed anteriorly between the body and the surface coil. Mechanical shear waves at 60 Hz were generated in the upper abdomen using an active driver system located outside the MRI room [4,20]. Either a rigid or flexible passive driver secured against the right chest wall was used to transmit mechanical vibrations from the active transducer into the body. For maximal driver-body contact, the rigid driver was placed on the right anterior chest wall while the flexible driver was placed on the right lateral chest wall [19]. The rigid driver is the standard device used in the FDA-cleared commercially available implementation of MRE technology. The flexible driver is an investigational prototype [19,25]. Three experienced MRI technologists performed the MRE exams in this study and, for any given subject, the same technologist performed both exams.

The propagating shear waves were imaged with a motion-sensitized imaging sequence at either end-inspiration or end-expiration. A gradient-recalled echo (GRE) sequence was used for 2D MRE acquisitions, and a spin-echo echoplanar imaging (SE-EPI) sequence was used for 3D MRE acquisitions [20,22]. 2D MRE acquired four axial slices through the widest portion of the liver in four separate breath-holds, and for each slice, magnitude and phase images were acquired for four equally spaced phases of the shear wave cycle. 3D MRE acquired 28 to 32 axial slices through the entire liver in 3 breath-holds, and, for each slice, magnitude and phase images were acquired for three equally spaced phases of the wave cycle. Acquisition parameters are listed in Table 1. 2D MRE acquisitions produced one set of wave images depicting displacement of the shear wave along the z-direction, while 3D MRE acquisitions produced three sets of wave images, each set depicting displacements along a different orthogonal direction (i.e., x, y, and z-directions). Subsequently, a 2D or 3D elastogram, depicting the estimated stiffness value for each pixel, was generated by analyzing all the wave images from the corresponding GRE or SE-EPI image acquisition, using a 2D or 3D inversion algorithm, respectively [20], [28], [29]. In addition, for 2D MRE, a confidence map was generated depicting pixel-by-pixel the goodness-of-fit (i.e., R^2) of the wave images to a smooth polynomial [30]. The values of the confidence map ranged from 0 to 1, with the latter indicating high quality wave data [30]. Confidence maps were not available for the investigational version of 3D MRE used in our study.

MRE Analysis

The magnitude, phase, wave, and elastographic images were transferred offline and analyzed using a custom software package (MRE Quant, Mayo Clinic, Rochester, MN). For each of the 72 2D-MRE scans and each of the 72 3D-MRE scans selected in random order, one image analyst (KW) drew ROIs in the liver on each reconstructed magnitude image [4,31]. The analyst was aware of whether the images were generated using 2D MRE or 3D MRE, but was blinded to the acquisition conditions (driver type, respiratory phase), exam order (first or second), and locations of ROIs on other scans for the same subject. ROIs were co-

localized automatically to the corresponding wave images and then modified to include only areas with adequate wave amplitude and relatively free of wave interference [31]. For 2D MRE, the final ROIs were created by excluding values not meeting the R^2 threshold of 0.95 on the confidence map. For 3D MRE, the final ROIs were created by taking the union of the ROIs drawn on the three sets of orthogonal wave images [27].

For each MRE scan, a single composite liver stiffness value was defined as the median stiffness value of all pixels in each ROI in all slices. Although previous investigators have used either the mean or the median per-pixel stiffness values, we used the median stiffness values because they are more robust against outliers. The cumulative liver ROI size for each scan was recorded as a quantitative surrogate of wave-image quality.

Statistical Analysis

Liver stiffness values and liver ROI sizes for 2D and 3D MRE under each condition were summarized descriptively.

Repeatability of 2D and 3D MRE under different conditions—Measurement repeatability between exams was assessed for both 2D and 3D MRE under each of the four conditions using the following statistical metrics proposed by the quantitative imaging biomarker alliance (QIBA) [11]:

Bias = mean difference between two repeated measurements Repeatability coefficient (RC) = 1.96 times the standard deviation for the difference between two repeated measurements taken under identical conditions

Limit of agreement (LOA) = bias ± RC Intraclass correlation coefficient (ICC) = ratio of between-subject variance to the sum of between- and within-subject variance

A 95% confidence interval was computed for each ICC. Significance of bias was tested with a one-tail t-test.

Reproducibility of 2D and 3D MRE under different conditions—Reproducibility was assessed for both 2D and 3D MRE performed under the following paired conditions:

Reproducibility of measurements made with different breath-hold phases (end-inspiration, end-expiration) while holding driver type (flexible, rigid) constant.

Reproducibility of measurements made with different driver types (rigid, flexible) while holding breath-hold phase (end-inspiration, end-expiration) constant.

As proposed by QIBA, the following metrics were used to evaluate reproducibility [11]:

Bias

Reproducibility coefficient (RDC)

Limit of agreement (LOA)

Concordance correlation coefficient (CCC)

These reproducibility metrics are analogous to the repeatability metrics, except they account for the variations between the paired conditions under evaluation [11]. As before, the 95%

confidence interval was computed for each CCC. Significance of bias was tested with a one-sample t-test.

2D and 3D ROI Size as a Surrogate of Wave-Image Quality—Because MRE-based stiffness estimation is derived from the wavelength of the imaged shear waves, wave-image quality is an important factor for its accuracy. In the current practice, a trained image analyst places an ROI on the elastogram of the liver to include regions of uniform waves without significant interference, so the ROI size represents the region of the liver with shear waves of adequate quality for reliable stiffness estimation. Thus, ROI size represents a practical, albeit subjective, surrogate for wave-image quality.

For both 2D and 3D MRE, ROI size was modeled as a function of breath-hold phase, driver type and their interaction using a linear mixed effect (LME) model. A random (subject-specific) intercept was fitted to adjust for within-subject dependence. The difference in ROI size between breath-hold phases and driver types for 2D and 3D MRE was estimated from the LME model.

All statistical analyses were performed using "R" statistical computing software (version 3.1.2 (2014-10-31) R: A language and environment for statistical computing. R Foundation for Statistical Computing, Vienna, Austria).

RESULTS

Representative images of 2D and 3D MRE are shown in Figures 1 and 2, respectively. Note that there is one set of wave images for 2D MRE (representing displacements along the z-direction) and three sets of wave images for 3D MRE (representing displacements along the x-, y-, and z-directions). Comparing the elastograms between row 1 (rigid driver and end-inspriation) and row 2 (flexible driver and end-inspiration) in Figure 1, we noted a moderate increase in stiffness at the posterior margin of the liver. This is a known artifact in 2D MRE, in which overestimation of stiffness values can be seen occasionally at the boundary of the organ imaged[22].

Liver Stiffness Values

2D and 3D MRE liver stiffness values measured under various conditions are plotted in Figure 3, with the median values overlain. Under all conditions, liver stiffness values tended to be higher (greater cohort median) and more variable (wider cohort interquartile range) for 2D than 3D MRE. For both 2D and 3D MRE, liver stiffness values tended to be higher and more variable at end-inspiration than at end-expiration, regardless of driver type. By comparison, stiffness values measured using rigid and flexible drivers were similar, regardless of breath-hold phase. Statistical comparisons were not made.

Repeatability of 2D and 3D MRE Under Various Conditions

The repeatability of 2D and 3D MRE liver stiffness values measured under various conditions is summarized in Table 2 and Figure 5. RCs and ICCs for 2D MRE range between 0. 29 – 0.49 and 0.71 – 0.91 respectively. RCs and ICCs for 3D MRE range between 0.16 – 0.26 and 0.84 – 0.96 respectively. Although the nominal RCs were slightly

higher and the nominal ICCs were slightly lower for 2D MRE than 3D MRE, formal pairwise comparisons of these 2D and 3DMRE parameters were not performed.

Expiration-vs.-Inspiration Reproducibility of 2D and 3D MRE

The reproducibility of 2D and 3D MRE liver stiffness values measured under different respiratory phases is summarized in Table 3 and Figure 6. Regardless of driver type, stiffness tended to be lower at end-expiration than end-inspiration for both 2D and 3D MRE, with the biases statistically significant and more pronounced for 3D (−0.13 ~ −0.19 kPa, depending on driver) than for 2D (−0.07 ~ – 0.08 kPa). Expiration -vs. -inspiration RDCs were slightly greater for 2D MRE (0.44–0.54, depending on driver) than for 3D MRE (0.30–0.31).; CCCs were modest for both techniques (0.71–0.72 for 2D MRE; 0.61–0.73 for 3D MRE).

Rigid-vs.-Flexible Driver Reproducibility of 2D and 3D MRE

The reproducibility of 2D and 3D MRE liver stiffness values measured using different driver types is summarized in Table 4 and Figure 7. For both 2D and 3D MRE, stiffness values were not meaningfully affected by driver type, regardless of breath-hold phase. Inter-driver biases were small (absolute values ≤ 0.07 kPa) and not statistically significant. Interdriver RDCs and CCCs ranged between 0.10–0.44 and 0.79–0.94, respectively. Nominally, measurements with different drivers were slightly more reproducible for 3D MRE than for 2D MRE, but the differences were not formally compared.

ROI Size (Wave Quality) for 2D and 3D MRE under Various Conditions

ROI sizes for 2D and 3D MRE under different conditions are plotted in Figure 4, with median ROI sizes overlain. 2D MRE and 3D MRE were not comparable because of differences in the number of acquired slices. Hence, the y-axes are scaled differently. As summarized in Table 5, 2D MRE ROI size was 10.9 cm^2 (15%) larger at expiration than inspiration ($p = 0.01$) in the LME model; 2D MRE ROI size was not significantly affected by driver type (difference of 2.3%, $p = 0.69$), and 3D MRE ROI size was not significantly affected by respiratory phase or driver type (differences of −4.4% and 8.4%, $p = 0.42$ and 0.11) in the LME model. There was no significant interaction between driver type and respiratory phase, so an interaction term was not included in the final LME model.

DISCUSSION

Key Findings

In this preliminary study, repeatability and reproducibility of 2D and 3D MRE under four conditions were evaluated in a small cohort of healthy adult volunteers. 2D MRE is potentially repeatable (RC = 0.29–0.36, ICC = 0.86–0.91) under all conditions except for rigid driver at end-inspiration (RC = 0.49, ICC = 0.71). 3D MRE is also potentially highly repeatable under all conditions (RC = 0.16–0.26, ICC = 0.84–0.96). Reproducibility for measurements made in different breath-hold phases was imperfect. A bias was observed, with stiffness values higher at endinspiration than end-expiration, and the differences were significant for 3D MRE. Breath-hold phase also contributed to measurement variability, as evidenced by the modest inspiration -vs. -expiration RDCs (0.30–0.54) and CCCs (0.61–0.72). In keeping with these observations, the interquartile range of stiffness values across

the cohort was wider for end-inspiratory than end-expiratory measurements. By comparison, measurements with different drivers are likley reproducible, and no significant bias was found between driver types. Additionally, variability was acceptable, with generally low RDCs (0.10–0.44) and high CCCs (0.79–0.94). Under all conditions, liver stiffness values tended to be higher for 2D than 3D MRE.

Interpretation of results

2D MRE performed at end-expiration using a rigid driver is the technique currently available for clinical use. The high interexamination ICC (0.86) observed in our study for this technique is consistent with previously reported results (ICC ~ 0.85 – 0.94; [13,14,17,32]). The other MRE technical variants examined in this study have not been described as extensively in the literature[33]. Our study suggests that most of these variants – including 2D MRE using a flexible driver at end-inspiration, and 3D MRE under any tested condition – are likely to have good repeatability. Repeatability was worse for 2D MRE using a rigid driver at end-inspiration.

We detected a small but significant bias between end-expiration and end-inspiration using 3D MRE, with stiffness estimates being greater at end-inspiration. This bias suggests that inspiration transiently increases liver stiffness in healthy adults. Although our study was not designed to examine the mechanism, a plausible explanation is that the liver experiences different static deformation between end-inspiration and end-expiration and hence results in different stiffness due to nonlinearity in tissue elasticity. This can also potentially explain the high variability in stiffness estimates between healthy adults at end-inspiration because individuals differ in their end-inspiratory capacity, thus resulting in variable changes in stiffness. The bias was not significant using 2D MRE, possibly because the slightly greater variability of 2D-MRE stiffness measurements reduced the power to detect a small but true effect, especially with our small sample size. Our finding suggests that breath-hold phase is potentially a confounding factor for hepatic stiffness measurements. Thus, we don’t recommend comparing stiffness measurements at different breath-hold phases. In the future, it will be interesting to evaluate MRE-based hepatic stiffness measurements throughout the respiratory cycle in order to understand the complete nonlinear relationship between the imposed strain and hepatic stiffness, which might provide a more comprehensive and robust evaluation of the biomechanics of hepatic tissues.

We detected no statistically significant bias between the two driver types. With the exception of 2D MRE at end-inspiration, RDCs (~ 0.19 – 0.37) between driver types were comparable to RCs (~ 0.20 – 0.36) for repeated estimates. These finding are consistent with other reproducibility studies on the two drivers in a cohort of volunteers as well as patients with different fibrosis stages (no statistically significant bias; RDC ~ 0.5) [19,25].

As expected, hepatic stiffness estimates for 2D MRE were slightly higher than those for 3D MRE when performed appropriately [22,27]. Hepatic 2D MRE is typically performed at the widest cross-section of the liver, in which the shear waves tend to propagate parallel to the axial-imaging plane, so the assumption of the simplified 2D inversion model is approximately valid [22,27]. However, this is not always true. Shear waves might travel obliquely at the boundaries of an organ, resulting in a longer apparent wavelength when

using a 2D inversion model, so hepatic 2D MRE may overestimate the stiffness value in these regions [22,27]. One such example is the posterior margin of the liver shown in Figure 1 (row 2) [27,34].This overestimation does not meaningfully affect the accuracy of 2D MRE for predicting fibrosis compared to histology, however, as these regions of erroneous stiffness measurements are excluded during ROI analysis [5,6].

Technical Implications

2D and 3D MRE is potentially repeatable under most conditions [13,14,32]. This suggests that newer MRE variants potentially can be suitable for longitudinal stiffness monitoring, but larger studies are required to validate these preliminary results. Stiffness tended to be higher and more variable at end-inspiration than at end-expiration, suggesting that breath-hold phase might be an important confounding factor in MRE-based hepatic stiffness measurements, as discussed earlier. Although not tested in our study, this higher variability would be expected to reduce the accuracy for fibrosis staging cross-sectionally using population-based cutoff values and for monitoring longitudinally. If patients can tolerate only end-inspiratory breath-holding, however, users should be aware that the published 2D MRE cut-offs for fibrosis staging do not apply, as they were developed with end-expiratory scanning, which measures stiffness at a different hepatic strain state. Because interdriver variability was small and there was no statistically significant bias between the two drivers, liver stiffness measurements using both drivers are likely equivalent. 2D- and 3D-MRE liver measurements differ, indicating that stiffness values collected with the two methods cannot be pooled. Informally, 3D MRE provided slightly higher repeatability (lower RCs, higher ICCs) than 2D MRE, regardless of driver type or breath-hold phase. These results should not be interpreted as indicating that 3D MRE is inherently superior to 2D MRE, however, as the difference may simply reflect more extensive liver sampling by the greater number of 3D MRE slices or differences in the details of the 2D and 3D pulse sequences and inversion algorithms. To more meaningfully compare of 2D vs. 3D MRE, future work should control for the number of slices, but this was outside the scope of our preliminary study.

Limitations

Our preliminary study was limited by small sample size, which creates moderate uncertainty in the statistical estimate of the repeatability and reproducibility metrics and prevents formal statistical comparisons of repeatability metrics for different methods and conditions. Our study cohort consisted of healthy adults, which limits generalizability to adults with liver disease, to obese individuals, and to children. We did not randomize the order in which MRE scans were performed, thus potential biases related to scanning order cannot be excluded. Further investigation of these methods and conditions is warranted in larger cohorts of adult and pediatric patients with chronic liver disease of variable etiology and severity and spanning a range of body habitus.

CONCLUSION

This preliminary study in healthy adults suggests that hepatic 2D and 3D MRE is potentially repeatable under all conditions. In addition, hepatic stiffness measurements with rigid and flexible driver are likely to be reproducible, and respiratory phase might be an important

confounding factor in MRE-based hepatic stiffness measurements. The study results are consistent with the standard recommendation that MRE acquisition be performed at end-expiration, as this state reduces measurement variability.

Acknowledgments

Funding: The study was partially supported by the following grants from the National Institutes of Health: R01DK088925, R56DK090350, R01EB001981, R01EB017197, and TL1TR00098. The content is solely the responsibility of the authors and does not necessarily represent the official views of the NIH.

References

1. Muthupillai R, Lomas D, Rossman P, Greenleaf J, Manduca A, Ehman R. Magnetic resonance elastography by direct visualization of propagating acoustic strain waves. Science. 1995; 269:1854–1857. DOI: 10.1126/science.7569924 [PubMed: 7569924]
2. Manduca A, Oliphant TE, Dresner MA, Mahowald JL, Kruse SA, Amromin E, et al. Magnetic resonance elastography: non-invasive mapping of tissue elasticity. Med Image Anal. 2001; 5:237–254. [PubMed: 11731304]
3. Muthupillai R, Rossman PJ, Lomas DJ, Greenleaf JF, Riederer SJ, Ehman RL. Magnetic resonance imaging of transverse acoustic strain waves. Magn. Reson. Med. 1996; 36:266–274. DOI: 10.1002/mrm.1910360214 [PubMed: 8843381]
4. Yin M, Talwalkar JA, Glaser KJ, Manduca A, Grimm RC, Rossman PJ, et al. Assessment of Hepatic Fibrosis With Magnetic Resonance Elastography. Clinical Gastroenterology and Hepatology. 2007; 5:1207–1213.e2. DOI: 10.1016/j.cgh.2007.06.012 [PubMed: 17916548]
5. Loomba R, Wolfson T, Ang B, Booker J, Behling C. Magnetic resonance elastography predicts advanced fibrosis in patients with nonalcoholic fatty liver disease: a prospective study. Hepatology. 2014; 60(6):1920–1928. [PubMed: 25103310]
6. Yin M, Talwalkar JA, Glaser KJ, Venkatesh SK, Chen J, Manduca A, et al. Dynamic postprandial hepatic stiffness augmentation assessed with MR elastography in patients with chronic liver disease. AJR Am J Roentgenol. 2011; 197:64–70. DOI: 10.2214/AJR.10.5989 [PubMed: 21701012]
7. Huwart L, Sempoux C, Salameh N, Jamart J, Annet L, Sinkus R, et al. Liver Fibrosis: Noninvasive Assessment with MR Elastography versus Aspartate Aminotransferase–to-Platelet Ratio Index. Radiology. 2007; 245:458–466. DOI: 10.1148/radiol.2452061673 [PubMed: 17940304]
8. Salameh N, Peeters F, Sinkus R, Abarca-Quinones J, Annet L, ter Beek LC, et al. Hepatic viscoelastic parameters measured with MR elastography: correlations with quantitative analysis of liver fibrosis in the rat. J Magn Reson Imaging. 2007; 26:956–962. DOI: 10.1002/jmri.21099 [PubMed: 17896384]
9. Huwart L, Sempoux C, Vicaut E, Salameh N, Annet L, Danse E, et al. Magnetic Resonance Elastography for the Noninvasive Staging of Liver Fibrosis. Gastroenterology. 2008; 135:32–40. DOI: 10.1053/j.gastro.2008.03.076 [PubMed: 18471441]
10. Loomba R, Sirlin CB, Ang B, Bettencourt R, Jain R. Ezetimibe for the treatment of Nonalcoholic steatohepatitis: assessment by novel magnetic resonance imaging and magnetic resonance elastography in a randomized trial (MOZART Trial). Hepatology. 2014; 61:1239–1250.
11. Raunig DL, McShane LM, Pennello G, Gatsonis C, Carson PL, Voyvodic JT, et al. Quantitative imaging biomarkers: A review of statistical methods for technical performance assessment. Stat Methods Med Res. 2015; 24:27–67. DOI: 10.1177/0962280214537344 [PubMed: 24919831]
12. Kessler LG, Barnhart HX, Buckler AJ, Choudhury KR, Kondratovich MV, Toledano A, et al. The emerging science of quantitative imaging biomarkers terminology and definitions for scientific studies and regulatory submissions. Stat Methods Med Res. 2015; 24:9–26. DOI: 10.1177/0962280214537333 [PubMed: 24919826]
13. Shire NJ, Yin M, Chen J, Railkar RA, Fox-Bosetti S, Johnson SM, et al. Test-retest repeatability of MR elastography for noninvasive liver fibrosis assessment in hepatitis C. J Magn Reson Imaging. 2011; 34:947–955. DOI: 10.1002/jmri.22716 [PubMed: 21751289]

14. Hines CDG, Bley TA, Lindstrom MJ, Reeder SB. Repeatability of magnetic resonance elastography for quantification of hepatic stiffness. J Magn Reson Imaging. 2010; 31:725–731. DOI: 10.1002/jmri.22066 [PubMed: 20187219]
15. Venkatesh SK, Wang G, Teo LLS, Ang BWL. Magnetic resonance elastography of liver in healthy asians: Normal liver stiffness quantification and reproducibility assessment. J Magn Reson Imaging. 2013; 39:1–8. DOI: 10.1002/jmri.24084 [PubMed: 24123300]
16. Lee YJ, Lee JM, Lee JE, Lee KB, Lee ES, Yoon J-H, et al. MR elastography for noninvasive assessment of hepatic fibrosis: reproducibility of the examination and reproducibility and repeatability of the liver stiffness value measurement. J Magn Reson Imaging. 2014; 39:326–331. DOI: 10.1002/jmri.24147 [PubMed: 23589232]
17. Shi Y, Guo Q, Xia F, Sun J, Gao Y. Short- and midterm repeatability of magnetic resonance elastography in healthy volunteers at 3.0T. Magnetic Resonance Imaging. 2014; 32:665–670. DOI: 10.1016/j.mri.2014.02.018 [PubMed: 24650683]
18. Weaver JB, Van Houten EEW, Miga MI, Kennedy FE, Paulsen KD. Magnetic resonance elastography using 3D gradient echo measurements of steady-state motion. Med. Phys. 2001; 28:1620–1628. DOI: 10.1118/1.1386776 [PubMed: 11548931]
19. Chen, J., Stanley, D., Glaser, K., Yin, M. Ergonomic flexible drivers for hepatic MR elastography. 18th Annual Meeting of International Society for Magnetic Resonance in Medicine; Stockholm, Sweden. 2010.
20. Yin M, Grimm RC, Manduca A. Rapid EPI-based MR elastography of the liver, in: 2006.
21. Sack I, Beierbach B, Hamhaber U, Klatt D, Braun J. Non-invasive measurement of brain viscoelasticity using magnetic resonance elastography. NMR Biomed. 2008; 21:265–271. DOI: 10.1002/nbm.1189 [PubMed: 17614101]
22. Hamhaber U, Sack I, Papazoglou S, Rump J, Klatt D, Braun J. Three-dimensional analysis of shear wave propagation observed by in vivo magnetic resonance elastography of the brain. 2007; 3:127–137. DOI: 10.1016/j.actbio.2006.08.007
23. Papazoglou S, Hamhaber U, Braun J, Sack I. Algebraic Helmholtz inversion in planar magnetic resonance elastography. Phys Med Biol. 2008; 53(12):3147. [PubMed: 18495979]
24. Morisaka H, Motosugi U, Glaser KJ, Ichikawa S, Ehman RL, Sano K, et al. Comparison of diagnostic accuracies of two- and three-dimensional MR elastography of the liver. J Magn Reson Imaging. 2016; 45:1163–1170. DOI: 10.1002/jmri.25425 [PubMed: 27662640]
25. Chen J, Glaser K, Yin M, Talwalkar J, Rossman PJ, Venkatesh SK, et al. Hepatic MR Elastography by Using Optimized Flexible Drivers. Proceeding of the Joint Annual Meeting ISMRM-ESMRMB. 2014:1–1.
26. Murphy IG, Graves MJ, Reid S, Patterson AJ, Patterson I, Priest AN, et al. Comparison of breath-hold, respiratory navigated and free-breathing MR elastography of the liver. Magnetic Resonance Imaging. 2017; 37:46–50. DOI: 10.1016/j.mri.2016.10.011 [PubMed: 27746391]
27. Shi Y, Glaser KJ, Venkatesh SK, Ben-Abraham EI, Ehman RL. Feasibility of using 3D MR elastography to determine pancreatic stiffness in healthy volunteers. J Magn Reson Imaging. 2014; 41:369–375. DOI: 10.1002/jmri.24572 [PubMed: 24497052]
28. Oliphant TE, Manduca A, Ehman RL, Greenleaf JF. Complex-valued stiffness reconstruction for magnetic resonance elastography by algebraic inversion of the differential equation. Magn. Reson. Med. 2001; 45:299–310. DOI: 10.1002/1522-2594(200102)45:2<299::AID-MRM1039>3.0.CO;2-O [PubMed: 11180438]
29. Manduca A, Lake DS, Kruse SA, Ehman RL. Spatio-temporal directional filtering for improved inversion of MR elastography images. Med Image Anal. 2003; 7:465–473. [PubMed: 14561551]
30. Dzyubak B, Glaser K, Yin M, Talwalkar J, Chen J, Manduca A, et al. Automated liver stiffness measurements with magnetic resonance elastography. J Magn Reson Imaging. 2013; 38:371–379. DOI: 10.1002/jmri.23980 [PubMed: 23281171]
31. Yin M, Glaser KJ, Talwalkar JA, Chen J, Manduca A, Ehman RL. Hepatic MR Elastography: Clinical Performance in a Series of 1377 Consecutive Examinations. Radiology. 2015; : 142141.doi: 10.1148/radiol.2015142141

32. Lee DH, Lee JM, Han JK, Choi BI. MR elastography of healthy liver parenchyma: Normal value and reliability of the liver stiffness value measurement. J Magn Reson Imaging. 2012; 38:1215–1223. DOI: 10.1002/jmri.23958 [PubMed: 23281116]

33. Trout AT, Serai S, Mahley AD, Wang H, Zhang Y, Zhang B, et al. Liver Stiffness Measurements with MR Elastography: Agreement and Repeatability across Imaging Systems, Field Strengths, and Pulse Sequences. Radiology. 2016; 281:793–804. DOI: 10.1148/radiol.2016160209 [PubMed: 27285061]

34. Murphy MC, Huston J, Jack CR, Glaser KJ, Manduca A, Felmlee JP, et al. Decreased brain stiffness in Alzheimer's disease determined by magnetic resonance elastography. J Magn Reson Imaging. 2011; 34:494–498. DOI: 10.1002/jmri.22707 [PubMed: 21751286]

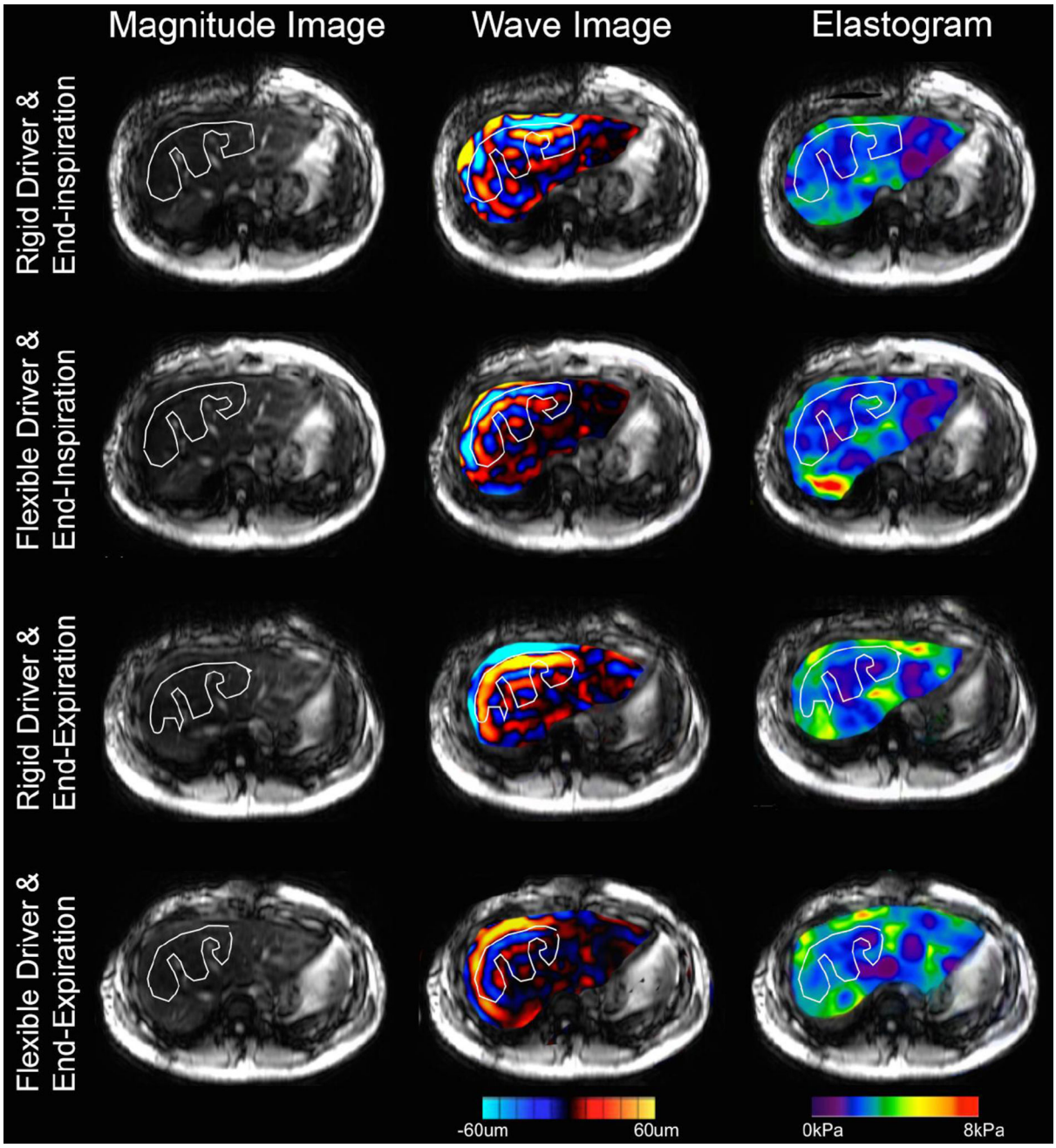

Figure 1.

Example of 2D MRE generated data for one subject at each combination of respiratory phase and driver type. Each row represents the magnitude image (left), wave image (middle), and elastogram (right) from one 2D MRE scan. For the wave image and the elastogram, only the region within the liver is shown and overlaid on the magnitude image for easier visualization. The white line represents the manually traced region of interest (ROI). The elastogram is color coded from purple to red for stiffness range from 0 to 8 kPa. The wave images are color coded with red in the positive direction and blue in the negative direction; the magnitude is coded by the brightness.

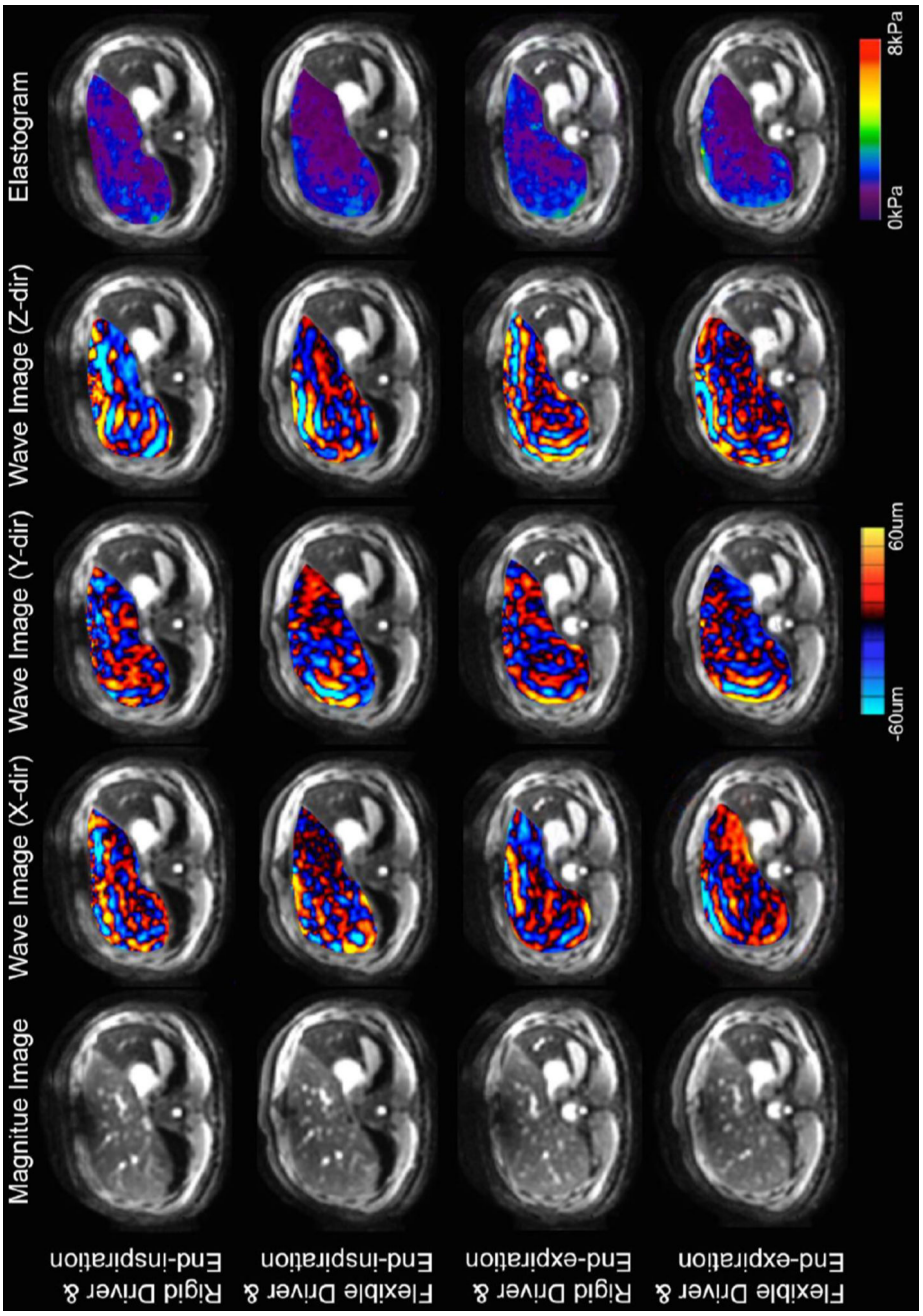

Figure 2.

Example of 3D MRE generated data for one subject at each combination of respiratory phase and driver type. Each row represents the magnitude image, elastogram, and three sets of wave image from one 3D MRE scan. The wave images depicted tissue displacements along the x-direction, y-direction, and z-direction respectively.

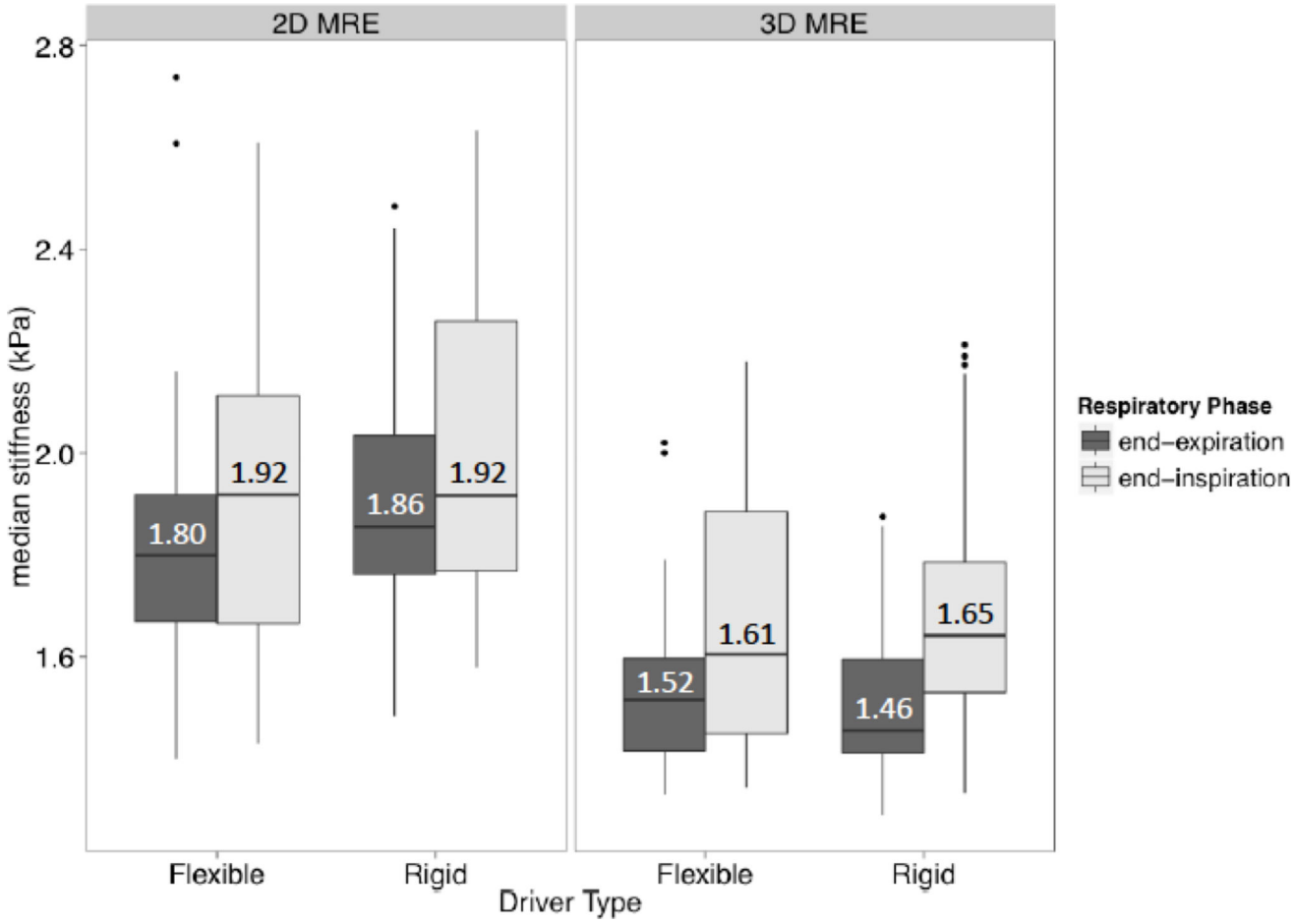

Figure 3.

Boxplots summarizing hepatic median stiffness estimates for 2D and 3D MRE under different conditions. For each MRE method, the boxplots are grouped by driver type (different columns) and then by breath-hold phase (different shading). Notice that measured stiffness values tend to be higher and slightly more variable for 2D MRE than 3D MRE under all conditions. Notice that stiffness values tend to be higher and more variable in inspiration than expiration, regardless of driver type, for both 2D and 3D MRE.

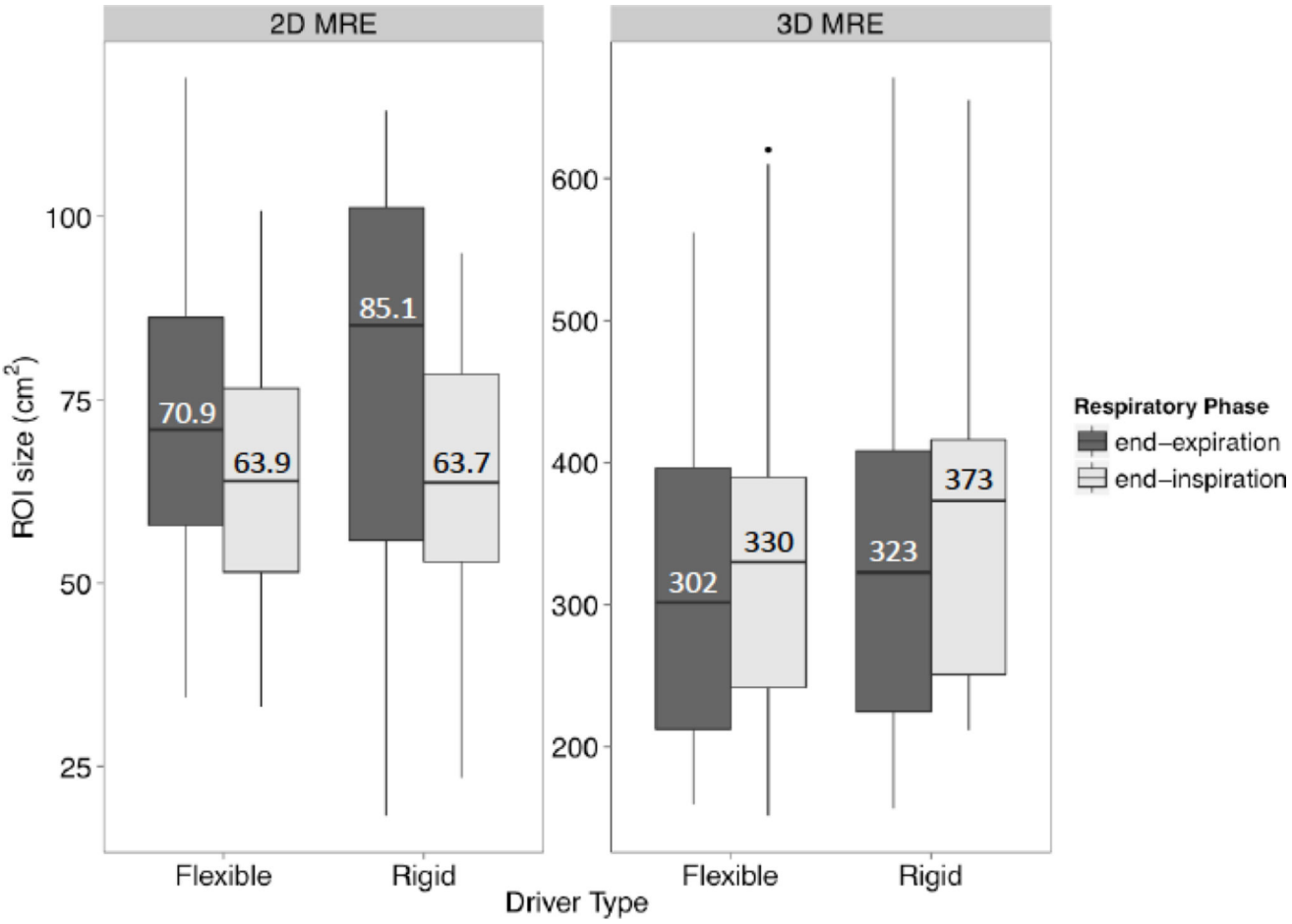

Figure 4.

Boxplots summarizing ROI sizes for 2D and 3D MRE under different conditions. For each MRE method, the boxplots are grouped by driver type (different columns) and then by breath-hold phase (different shading). ROI sizes between methods are not comparable due to differences in the numbers of acquired slices (4 for 2D MRE, 28–32 for 3D MRE).

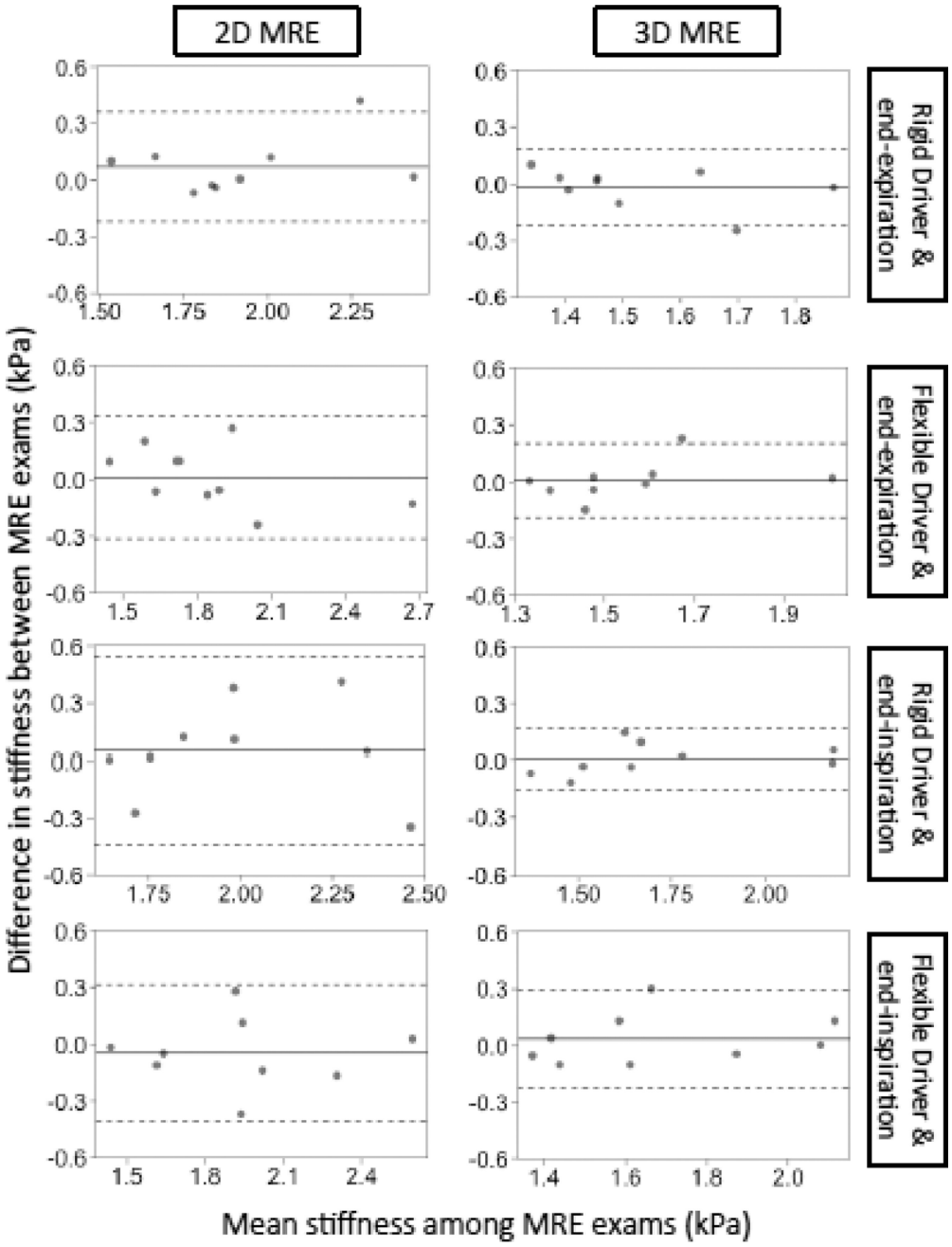

Figure 5.

Bland-Altman plots for the repeatability of 2D and 3D MRE under different conditions. The horizontal axis is the mean stiffness between exam 1 & 2 and the vertical axis is the difference in stiffness between exam 1 & 2. The dotted lines represent the interval of the limit of agreement (LOA) in Table 2.

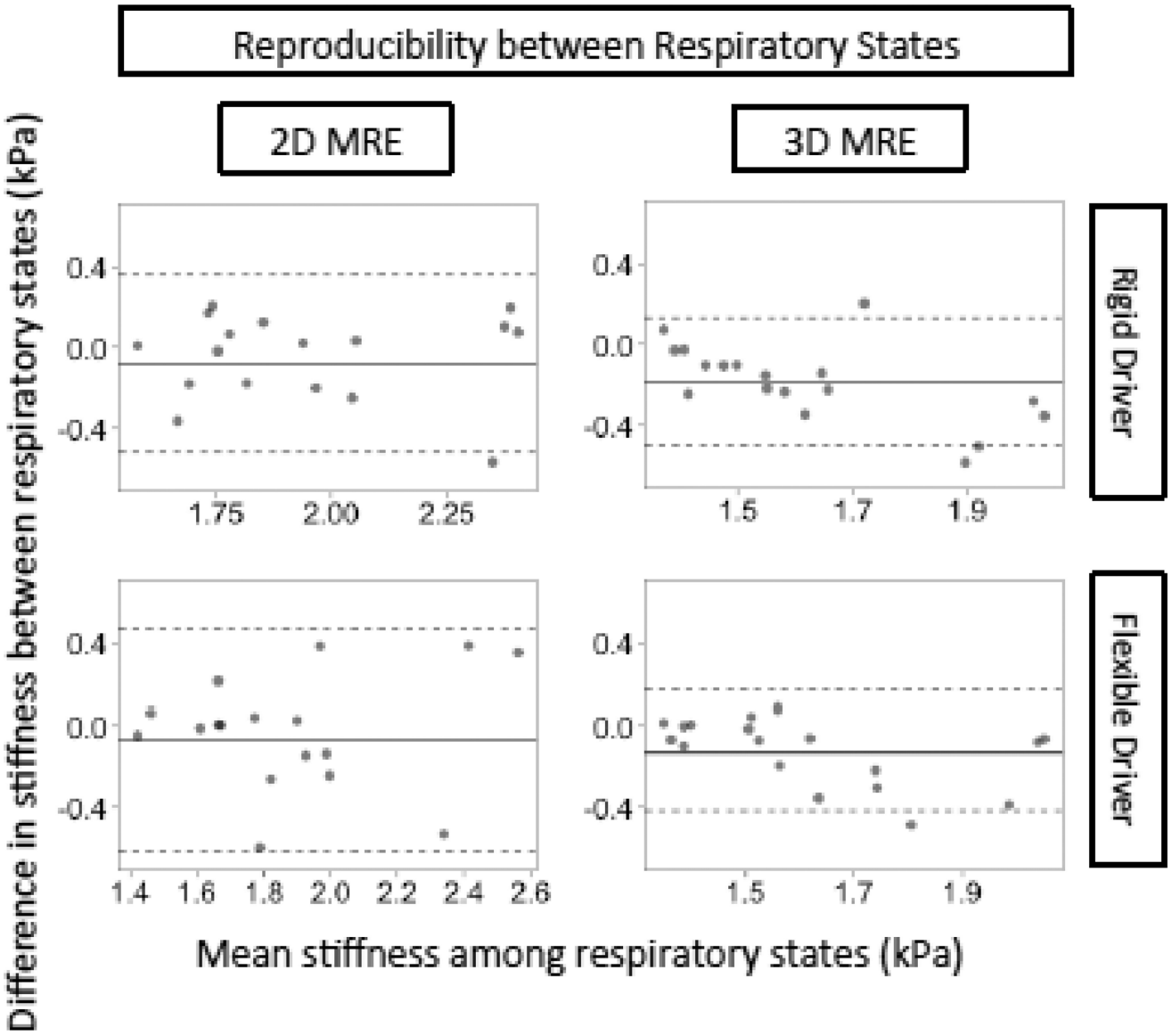

Figure 6.

Bland-Altman plots for the reproducibility of 2D and 3D MRE stiffness values measured under different breath-hold phases, keeping driver type constant. The horizontal axis is the mean stiffness between the two breath-hold phases and the vertical axis is the difference between the two breath-hold phases. The dotted lines represent the interval of the LOA in Table 3.

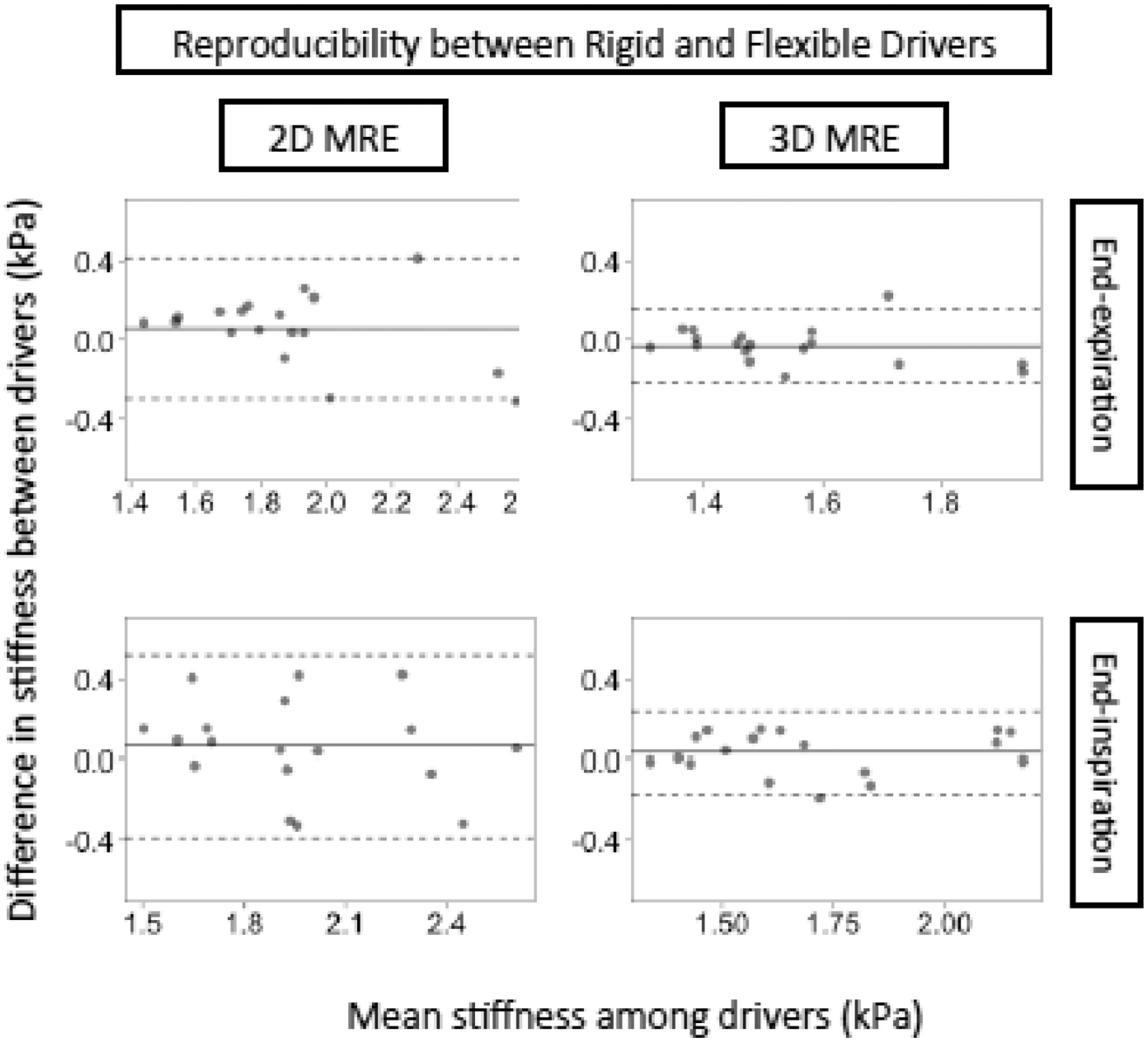

Figure 7.

Bland-Altman plots for the reproducibility of 2D and of 3D MRE stiffness values measured with different driver types, keeping breath-hold phase constant. The horizontal axis is the mean stiffness between the two drivers and the vertical axis is the difference in stiffness between the two drivers. The dotted lines represent the intervals of the LOA in Table 4.

Table 1

MRE acquisition parameters

	2D MRE	3D MRE
Pulse sequence	GRE	SE-EPI
Phase offsets	4	3
Slice Thickness	10 mm	3.5 mm
Interslice gap	0 mm	-
Number of slices	4	28 – 32
Motion-sensitization	z-direction	x,y,z-direction
Echo time (TE)	20.2	49.4
Repetition time (TR)	50	1333.8 ms
Flip angle (FA)	30°	90°
Image matrix	256 × 64	72 × 72
Field of view (FOV)	38 × 38 cm	44.8 × 44.8 cm
Number of signal averages	1	1
Parallel imaging acceleration factor	2	3
Bandwidth (BW)	±31.25 kHz	±250 kHz

GRE = Gradient-recalled echo; SE-EPI=spin-echo echo-planar imaging.

Table 2

Repeatability of 2D and 3D MRE stiffness values measured under various conditions

	Condition		Repeatability parameter			
MRE method	Breath-hold phase	Driver type	Bias (kPa)	RC	LOA (kPa)	ICC
2D *	Expiration	Rigid	0.07	0.29	−0.22, 0.36	0.86 (0.56, 0.96)
2D	Expiration	Flexible	0.01	0.33	−0.32, 0.34	0.91 (0.70, 0.98)
2D	Inspiration	Rigid	0.05	0.49	−0.44, 0.55	0.71 (0.22, 0.92)
2D	Inspiration	Flexible	−0.05	0.36	−0.41, 0.31	0.88 (0.61, 0.97)
3D	Expiration	Rigid	−0.02	0.20	−0.22, 0.19	0.84 (0.49, 0.96)
3D	Expiration	Flexible	0.01	0.20	−0.19, 0.21	0.90 (0.65, 0.97)
3D	Inspiration	Rigid	0.01	0.16	−0.16, 0.17	0.96 (0.86, 0.99)
3D	Inspiration	Flexible	0.03	0.26	−0.22, 0.29	0.90 (0.65, 0.97)

RC = Repeatability coefficient; LOA = limit of agreement; ICC = Intraclass coefficient of repeatability; ROI = Regions of Interests.

Values in parentheses are 95% confidence limits.

* This implementation of MRE is the FDA-approved clinically available implementation of MRE.

Table 3

Reproducibility of 2D and 3D MRE stiffness values measured under different breath-hold phases, keeping driver type constant

	Conditions		Reproducibility parameter				
MRE method	Breath-hold phase (Variable condition)	Driver type (Constant condition)	Bias (kPa)*	Bias p-value	RDC	LOA (kPa)	CCC
2D	Exp – Ins	Rigid	− 0.08	0.14	0.44	−0.52, 0.36	0.72 (0.38, 0.89)
2D	Exp – Ins	Flexible	− 0.07	0.28	0.54	−0.62, 0.47	0.71 (0.36, 0.88)
3D	Exp – Ins	Rigid	− 0.19	<0.01	0.31	−0.50, 0.13	0.61 (0.26, 0.81)
3D	Exp – Ins	Flexible	− 0.13	<0.01	0.30	−0.42, 0.17	0.73 (0.41, 0.89)

Table summarizes the reproducibility parameters for 2D and 3D MRE measured under different breath-hold phases, keeping driver type constant.

* The bias is calculated as the mean value in expiration minus the mean value in inspiration. Hence, a negative bias indicates that liver stiffness values measured in expiration were less than those measured in inspiration.

Ins=inspiration;. Exp=expiration;. RDC=reproducibility coefficients; LOA=Limit of Agreement; CCC=concordance correlation coefficients.

Values in parentheses are 95% confidence limits.

Table 4

Reproducibility of 2D and 3D MRE stiffness values measured with different driver types, keeping breath-hold phase constant

	Conditions		Reproducibility parameter				
MRE method	Breath-hold phase (Constant condition)	Driver type (Variable condition)	Bias (kPa)*	Bias p-value	RDC	LOA (kPa)	CCC
2D	Inspiration	Rigid – Flexible	0.07	0.22	0.44	−0.37, 0.50	0.79 (0.50, 0.92)
2D	Expiration	Rigid – Flexible	0.06	0.20	0.37	−0.31, 0.43	0.83 (0.58, 0.94)
3D	Inspiration	Rigid – Flexible	0.03	0.19	0.20	−0.17, 0.23	0.94 (0.82, 0.98)
3D	Expiration	Rigid – Flexible	−0.03	0.20	0.19	−0.22, 0.16	0.86 (0.65, 0.95)

Table summarizes the reproducibility parameters for 2D and 3D MRE measured with different drivers, keeping breath-hold phase constant.

* The bias is calculated as the mean stiffness value with the rigid driver minus the mean value with the flexible driver. Hence, a positive bias indicates that liver stiffness values measured with the rigid driver were greater than those measured with the flexible driver.

RDC=reproducibility coefficients; LOA=Limit of Agreement; CCC=concordance correlation coefficients.

Values in parentheses are 95% confidence limits.

Table 5

Relative ROI sizes under different conditions for 2D and 3D MRE

	2D MRE		3D MRE	
Condition	**Difference in ROI size**	**p-value**	**Difference in ROI size**	**p-value**
Expiration – inspiration	10.9 cm^2 (2.5, 19.3) 15.0% (3.4%, 25.6%)	0.01	−14.6 cm^2 (−50.1, 20.8) −4.4% (−15.2%, 6.3%)	0.42
Rigid – flexible driver	1.7 cm^2 (−6.7, 10.0) 2.3% (−9.5%, 14.2%)	0.69	29.5 cm^2 (−10.2, 61.7) 8.4% (−2.9%, 17.6%)	0.11

For 2D and 3D MRE, difference in sizes of ROIs drawn for different conditions (expiration vs. inspiration; rigid driver vs. flexible driver) were estimated using an LME model. Shown are the mean differences and their 95% confidence intervals (as well as the mean percent differences and their 95% confidence intervals). A positive mean difference means ROI size was larger in expiration or using the rigid driver, depending on the condition being modeled. There was no interaction between driver and respiratory phase. Percentage difference for expiration vs. inspiration is defined as (stiffness in expiration − stiffness in inspiration)/(stiffness in expiration). Percentage difference in stiffness between rigid vs. flexible driver is defined as (stiffness using rigid driver − stiffness using flexible driver)/(stiffness using rigid driver).